DALTON
FULL PAPER

Anion recognition by conservation of hydrogen-bonding patterns in salts of copper(II) co-ordinated by tetradentate bis(amidino-*O*-alkylurea) ligands†

Alexander J. Blake, Peter Hubberstey,* Unchulee Suksangpanya and Claire L. Wilson

School of Chemistry, University of Nottingham, University Park, Nottingham, UK NG7 2RD.
E-mail: Peter.Hubberstey@Nottingham.ac.uk

Received 28th April 2000, Accepted 23rd June 2000
First published as an Advance Article on the web 22nd September 2000

Refluxing 1,2-bis(2-cyanoguanidino)ethane (L^1) in methanol or ethanol containing copper(II) sulfate resulted in the formation of $[CuL^{3m}][MeOSO_3]_2$ $\{L^{3m} = [HN{=}C(OMe)NHC(NH_2){=}NCH_2]_2\}$ and $[CuL^{3e}][EtOSO_3]_2$ $\{L^{3e} = [HN{=}C(OEt)NHC(NH_2){=}NCH_2]_2\}$. Structural analysis of these complexes has revealed hydrogen-bonded supramolecular architectures constructed from $[CuL^i]^{2+}$ cations with square planar CuN_4 chromophores and $[ROSO_3]^-$ anions. The basic supramolecular synthon is a 1-D chain of alternating cations and anions, a motif which is also found with Cl^- and $[BF_2(OMe)_2]^-$ anions. The $[ROSO_3]^-$ anion is an ideal fit for the space between two cations; its hydrophobic *O*-alkyl group is surrounded by the *O*-alkyl groups of the cations and its hydrophilic SO_3^- moiety forms N–H · · · O hydrogen bonds with their amino and imino functionalities. In $[CuL^{3m}][MeOSO_3]_2$ the chains, which are linear, are hydrogen bonded through a second methyl sulfate anion to give a 2-D sheet motif. The sheets are bound together to form a 3-D framework through very weak Cu · · · O co-ordinative interactions which complete a tetragonally elongated octahedral geometry for the copper(II) centre. In $[CuL^{3e}][EtOSO_3]_2$ the chains, which are sinusoidal, are hydrogen bonded through a second ethyl sulfate anion to give a bilayered arrangement. The bilayers aggregate into a 3-D framework by a combination of hydrogen bonding and weak Cu · · · O co-ordinative interactions which result in a square pyramidal co-ordination geometry for the copper(II) centre. Despite the fit between $[CuL^i]^{2+}$ cations and alkyl sulfate anions in the chain, when a mixture of anions (chloride and ethyl sulfate) is present in the crystallisation medium, the preferred chain supramolecular synthon of the product, $[CuL^{3e}][EtOSO_3]Cl{\cdot}2H_2O$, is that containing chloride. The ethyl sulfate anions are involved, together with water molecules, in a complex hydrogen-bonding network which connects the chains into 2-D sheets, which are assembled, in turn, into a 3-D network structure by a combination of hydrogen bonding networks and exceedingly weak Cu · · · Cl co-ordinative interactions, which give rise to a square pyramidal copper(II) co-ordination geometry.

The field of crystal engineering in which transition metal cationic centres are linked through anions *via* hydrogen-bonded supramolecular synthons is receiving growing attention.[1,2] This work is driven by the elegant multi-dimensional architectures which can be fabricated by bringing together the rapidly maturing fields of hydrogen-bonded crystal engineering[3] and inorganic co-ordination polymer construction.[4] We have recently described[5] the creation of supramolecular architectures based on $[CuL^i]^{2+}$ (i = 3m, 3e, 4m or 4e; Scheme 1) cations in which the copper(II) centre is co-ordinated by tetradentate C_2- or C_3-linked bis(amidino-*O*-alkylurea) ligands which have extensive hydrogen-bonding potential (eight N–H donor centres and two oxygen acceptor centres; Scheme 2).

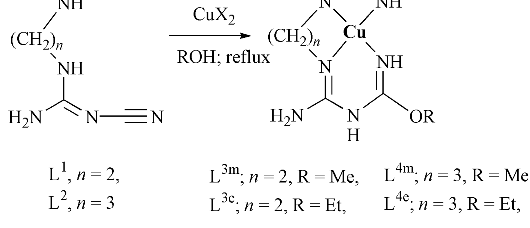

Scheme 1 Synthesis of $[CuL^i]^{2+}$ cations.

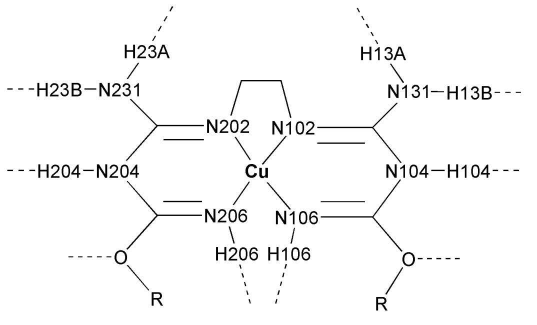

Scheme 2 Hydrogen-bonding potential of the $[CuL^i]^{2+}$ cation.

These cations are readily prepared by alcoholysis of the corresponding bis(2-cyanoguanidine) precursor ligands (L^1 or L^2; Scheme 1) in the presence of a copper(II) salt.

When using copper(II) chloride[5] the same building block, a hydrogen-bonded 1-D chain of alternating $[CuL^i]^{2+}$ cations and chloride anions (Scheme 3), is conserved in the complexes $[CuL^{3m}]_4[CuCl_4]Cl_6{\cdot}2H_2O$ **1**, $[CuL^{3e}]Cl_2{\cdot}2H_2O{\cdot}MeOH$ **2** and $[CuL^{4m}]Cl_2{\cdot}2H_2O$ **3**. A slightly modified motif, including a water molecule, occurs in $[CuL^{3m}]Cl_2{\cdot}2H_2O$ **4**. The chains are linked into sheets by hydrogen-bonding contacts involving

---

† Based on the presentation given at Dalton Discussion No. 3, 9–11th September 2000, University of Bologna, Italy.

Electronic supplementary information (ESI) available: rotatable 3-D crystal structure diagram in CHIME format. See http://www.rsc.org/suppdata/dt/b0/b003427o/

DOI: 10.1039/b003427o

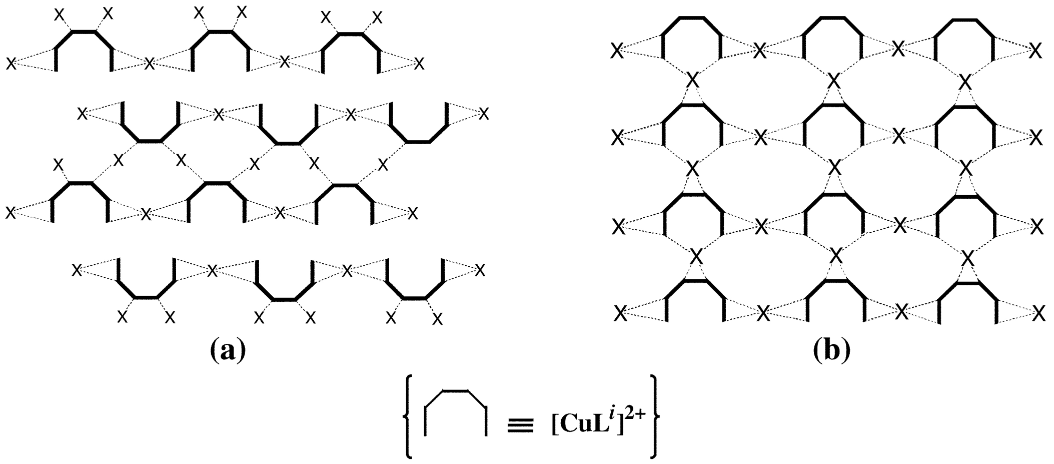

Scheme 3 Packing of chains to generate sheet structures. When linked *via* ribbons the cations in adjacent chains face in opposite directions (a) but when linked directly they face in the same direction (b).

anions and solvent molecules, either *via* formation of ribbons {**1**, **2** and **3**; Scheme 3(a)} or directly {**4**; Scheme 3(b)}. 3-D Frameworks result from a combination of elongated axial Cu···Cl co-ordinative contacts and complex hydrogen-bonding contacts again involving anions and solvent molecules.

Crystallisation, from methanol, of the products obtained with copper(II) tetrafluoroborate[5] revealed the formation of the $[BF_2(OMe)_2]^-$ anion in the complex with $[CuL^{3e}]^{2+}$, $[CuL^{3e}][BF_2(OMe)_2][BF_4]$ **5**, but not in the complex with $[CuL^{3m}]^{2+}$, $[CuL^{3m}][BF_4]_2$ **6**. It acts as a hydrogen-bonding acceptor in conjunction with the $[CuL^{3e}]^{2+}$ cation to generate 1-D chains similar to those conserved in the chloride structures **1**, **2** and **3**. The chains are directly linked into sheets by hydrogen-bonding contacts involving BF_4^- anions to give an architecture resembling that in **4** {Scheme 3(b)}.

We now report the extraordinary results obtained when using copper(II) sulfate as the template for the alcoholysis reaction and the anion recognition properties of the various hydrogen bonding sites of the $[CuL^i]^{2+}$ cations (Scheme 2). For both methanol and ethanol, esterification of sulfate occurs to give monoalkyl sulfate, in the complexes $[CuL^{3m}][MeOSO_3]_2$ **7** and $[CuL^{3e}][EtOSO_3]_2$ **8**, eqn. (1). As for $[BF_2(OMe)_2]^-$ formation,

$$[SO_4]^{2-} + ROH \rightleftharpoons [ROSO_3]^- + OH^- \ (R = Me \text{ or } Et) \qquad (1)$$

we believe the reaction is driven by the ability of alkyl sulfate to act as the hydrogen-bonding acceptor in the supramolecular synthon which generates the chain of alternating cations and anions.

Although the esterification reaction was unexpected, a subsequent literature search did reveal a single report describing the formation of the copper(I) complex $[CuL_2(PPh_3)_2][ROSO_3]$ (L = pyridine-2-thione or quinoline-2-thione; R = Me or Et) by reduction of copper(II) sulfate in alcoholic media containing the heterocyclic thione and tertiary phosphine.[6]

We have also assessed the anion recognition properties of the various hydrogen-bonding sites of the $[CuL^i]^{2+}$ cations by crystallisation of the mixed anion complex $[CuL^{3e}][EtOSO_3]Cl\cdot 2H_2O$ **9** from a mixture of $[CuL^{3e}][EtOSO_3]_2$ and $[CuL^{3e}]Cl_2\cdot 2H_2O$.

Results and discussion

The products of the alcoholysis of L^1 in the presence of copper(II) sulfate, $[CuL^i][ROSO_3]_2$ (i = 3m, R = Me, **7**; i = 3e, R = Et, **8**; Scheme 1), were provisionally characterised by analytical (C, H, N) and spectroscopic (IR, UV-visible and EPR) methods. Their UV-visible and EPR spectra were effectively identical and similar to those obtained for the corresponding halide and tetrafluoroborate salts inferring very similar chromophores for all complexes with C_2-linked ligands (Table 1). Subsequently, small, but well formed crystals of **7** and **8** were obtained by vapour phase diffusion of Et_2O into MeOH solutions. Similar crystallisation experiments with a mixture of the ethyl sulfate, $[CuL^{3e}][EtOSO_3]$, and chloride, $[CuL^{3e}]Cl_2\cdot 2H_2O$, gave crystals of the mixed anion compound $[CuL^{3e}][EtOSO_3]Cl\cdot 2H_2O$, **9**.

Table 1 Spectral data for the complexes obtained from alcoholysis of L^1 in the presence of copper(II) salts

Product	No.	UV-Visible λ_{max}/nm (ε/dm^3 mol^{-1} cm^{-1})	EPR data $g_{zz}/g_{yy}/g_{xx}$
$[CuL^{3m}]_4[CuCl_4]Cl_6\cdot 2H_2O$	**1**	550 (190) 839 (91)	2.19/2.07/1.97 2.29/2.10/2.03
$[CuL^{3m}]Cl_2\cdot 2H_2O$	**4**	550 (52)	2.19/2.05/1.96
$[CuL^{3m}]Br_2\cdot 2H_2O$	—	552 (56)	2.19/2.06/1.97
$[CuL^{3m}][BF_4]_2$	**6**	546 (54)	2.18/2.05/1.97
$[CuL^{3e}]Cl_2\cdot 2H_2O$	—	546 (61)	2.19/2.05/1.97
$[CuL^{3e}]Br_2$	—	550 (34)	2.19/2.06/1.98
$[CuL^{3e}][BF_4]_2$	—	546 (49)	2.19/2.06/1.97
$[CuL^{3m}][MeOSO_3]_2$	**7**	546 (61)	2.20/2.06/1.97
$[CuL^{3e}][EtOSO_3]_2$	**8**	543 (55)	2.20/2.06/1.97

Previously reported structural data for copper(II) alkyl sulfates are restricted to $[Cu(H_2O)_4(EtOSO_3)_2]$[7] and $[CuL_2(H_2O)_2][MeOSO_3]_2$ (L = bis(1-methylimidazol-2-yl) sulfide).[8] The structure of a single copper(I) alkyl sulfate $[CuL_2(PPh_3)_2][EtOSO_3]\cdot 0.5H_2O$ (L = quinoline-2-thione)[6] has been reported. Other structurally characterised transition metal alkyl sulfates include $[RuL_2][MeOSO_3]_2$ (L = tris(pyridin-2-yl)methanol)[9] and $[Rh(\eta^5\text{-}C_5H_5)(CH_3)(CO)(P^iPr_3)][MeOSO_3]$.[10] A number of nonaaqua lanthanide ethyl sulfates, $[Ln(H_2O)_9][EtOSO_3]_3$ (Ln = Y, Ce, Pr, Ho, Er or Yb),[11] have also structurally been characterised to assist interpretation of their magnetic and spectroscopic properties.[12]

Co-ordination geometries of the $[CuL^i]^{2+}$ cations

The $[CuL^i]^{2+}$ cations in the three complexes have a common CuN_4 square planar geometry, which is responsible for their almost identical UV-visible and EPR spectral data (Table 1). They differ, however, in the siting of anions in the remote axial sites. The three structures are compared in Fig. 1; pertinent interatomic distances and angles are collated in Table 2. In **7** oxygen atoms of two crystallographically independent methyl sulfate anions remotely occupy the axial sites {Cu···O 3.005(3), 3.240(3) Å} to give a tetragonally elongated octahedral arrangement {Fig. 1(a)}. In **8** only one axial site is occupied by a much less remote ethyl sulfate oxygen

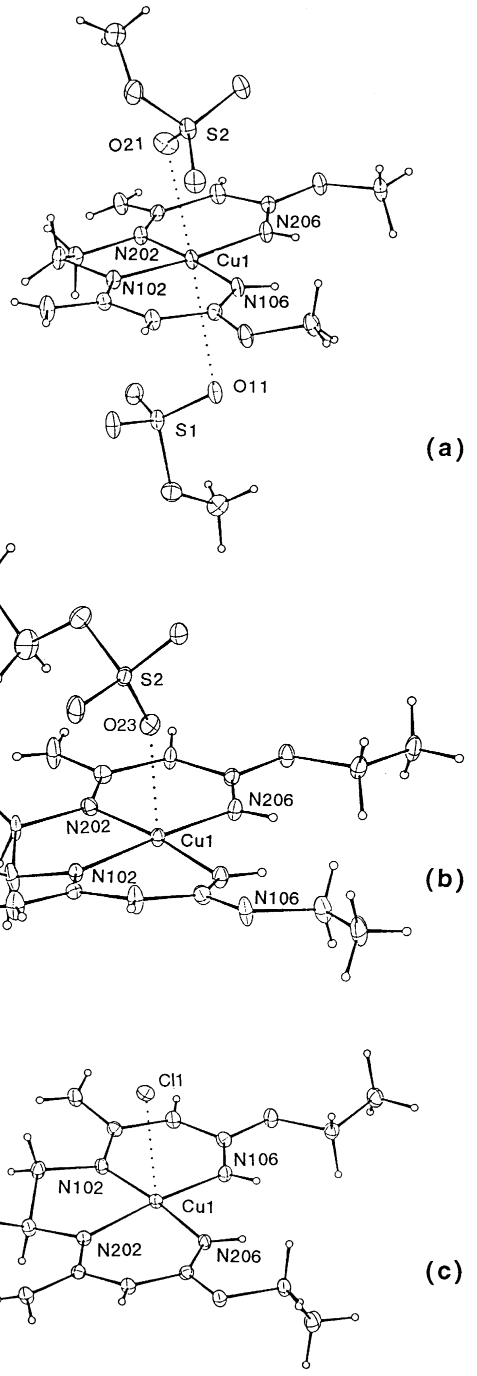

Fig. 1 Co-ordination geometries of the $[\mathrm{CuL}']^{2+}$ cations in (a) $[\mathrm{Cu}^{3m}][\mathrm{MeOSO_3}]_2$ **7**, (b) $[\mathrm{CuL}^{3e}][\mathrm{EtOSO_3}]_2$ **8** and (c) $[\mathrm{CuL}^{3e}][\mathrm{EtOSO_3}]\mathrm{Cl}\cdot 2\mathrm{H_2O}$ **9**.

atom {Cu···O 2.441(3) Å} giving a square pyramidal geometry {Fig. 1(b)}. A similar square pyramidal arrangement is found in **9** but the axially located chlorine anion {Cu···Cl 2.925(2) Å} is much more remote {Fig. 1(c)}. The identity and location of the axial anions have virtually no effect on the geometry of the $\mathrm{CuN_4}$ square plane as evidenced by the very limited variation in Cu···N distances (Table 2) and bite angles of the five- [N(102)–Cu–N(202); Table 2] and six-membered chelate rings [N(102)–Cu–N(106), N(202)–Cu–N(206); Table 2]. The dihedral angles between the two amidino-*O*-alkylurea moieties are also very similar lying between 6 and 7° (Table 2). These values, which confirm the near planarity of the $\mathrm{CuN_4}$ chromophore, are similar to those of the $\mathrm{C_2}$-linked cations in the chlorides (**1**, 0.0; **2**, 4.26; **4**, 6.11°) and tetrafluoroborates (**5**, 8.64; **6**, 5.24°) but are much smaller than those for the $\mathrm{C_3}$-linked cations in the chlorides (**3**, 26.88; 27.69°).

Hydrogen-bonded 1-D chain formation

Hydrogen-bonded chains, comprising alternating cations and anions, form the basis of the extended structures of all three compounds. The chain architectures are compared in Fig. 2; pertinent interatomic distances and angles are collated in Table 3. For the mixed anion complex, **9**, chloride anions bridge the cations to give an arrangement {Fig. 2(c)} identical to those found in **1**, **2** and **3** with comparable intrachain Cu···Cu separations (**9**, 12.708; **1**, 12.910; **2**, 12.677; **3**, 12.656 Å). The chains found in the alkyl sulfates, **7** {Fig. 2(a)} and **8** {Fig. 2(b)}, are similar but with much larger intrachain Cu···Cu separations (**7**, 14.157; **8**, 13.851 Å). The geometry of the anion is such that it fits between two cations, its hydrophobic *O*-alkyl moiety lying between the *O*-alkyl groups of the adjacent cations and its hydrophilic $\mathrm{SO_3}^-$ moiety sited such that all three oxygen atoms can act as hydrogen-bond acceptors for two pairs of N–H donors (N104, N131 and N204, N231) on adjacent cations {Fig. 2(a), 2(b)}. These are the same N–H donors as propagate the chains in **9** {Fig. 2(c)}. Although it appears from the structural diagram for **8** {Fig. 2(b)} that C–H···O hydrogen bonds exist between the methylene and methyl fragments of the *O*-alkyl units of the anions and the oxygen atoms of the *O*-alkyl units of the cations, their structural parameters (*e.g.*, C13···O251 3.48 Å, C13–H1D···O251 148°; C12···O151 3.50 Å, C12–H1B···O151 144°) are such that they must be considered to be extremely weak.

Hydrogen-bonded aggregation of chains into 2-D sheets in complexes 7 and 9

Although the alignment of the chains in complexes **7** and **9** is linear, that of the chains in **8** is sinusoidal, a difference which has ramifications in the construction of the overall network architecture. In **7** (Fig. 3) and **9** (Fig. 4) the chains align facing the same direction to form 2-D sheets. The link between chains in **7** is provided by a methyl sulfate anion hydrogen bonded on one side to the co-ordinated imino nitrogens (N106, N206) of a $[\mathrm{CuL}^{3m}]^{2+}$ cation and on the other to an amino nitrogen (N131) of a $[\mathrm{CuL}^{3m}]^{2+}$ cation in the next chain (Fig. 3). That between chains in **9** is more complex, involving water molecules as well as an ethyl sulfate anion. The anion is hydrogen bonded to the co-ordinated imino nitrogens (N106, N206) of a $[\mathrm{CuL}^{3e}]^{2+}$ cation in a similar fashion to that in **7** but the connection to the $[\mathrm{CuL}^{3e}]^{2+}$ cation in the next chain involves both amino nitrogens (N131, N231), which are hydrogen-bonded to the anion through separate water molecules (Fig. 4). Full details of the hydrogen bonds involved in the construction of the sheet structures are collected in Table 4.

Construction of 3-D frameworks for compounds 7 and 9

To understand the interactions linking the sheets into 3-D frameworks it is necessary to return to the copper(II) co-ordination geometries. The two weak Cu···O contacts which complete the tetragonally elongated octahedron in **7** {Fig. 1(a); Table 2} form the basis of the principal links between sheets (Fig. 5). The two bonding arrangements are depicted in Scheme 4. In both, two methyl sulfate anions form a centrosymmetric bridge between two $[\mathrm{CuL}^{3m}]^{2+}$ cations, forming a co-ordinate bond to the copper centre of the first cation and a pair of hydrogen bonds to the second cation. They differ in the type of N–H donors: in the first the co-ordinated imino {N106, N206; Scheme 4(a)} nitrogens, in the second, the amino/imino {N131/N104; Scheme 4(b)} pair. Additional cohesion is provided by a single N–H···O hydrogen bond between the amino nitrogen of the $[\mathrm{CuL}^{3m}]^{2+}$ cation (N231) and an oxygen atom (O23) of a methyl sulfate anion from an adjacent sheet (Fig. 5; Table 5). The intersheet Cu···Cu

Table 2 Pertinent interatomic distances (Å) and angles (°) in complexes **7**, **8** and **9**

	7	**8**	**9**
Cu–N(102)	1.938(2)	1.953(2)	1.955(2)
Cu–N(106)	1.947(2)	1.951(2)	1.959(2)
Cu–N(202)	1.958(2)	1.948(2)	1.957(2)
Cu–N(206)	1.958(2)	1.945(2)	1.959(2)
N(102)–Cu–N(106)	91.70(9)	90.45(8)	90.56(6)
N(102)–Cu–N(202)	84.42(9)	85.61(8)	84.63(6)
N(102)–Cu–N(206)	173.65(9)	173.58(9)	169.18(6)
N(106)–Cu–N(202)	175.71(9)	174.72(9)	174.59(5)
N(106)–Cu–N(206)	93.79(9)	92.72(8)	93.62(6)
N(202)–Cu–N(206)	90.19(9)	90.87(8)	90.70(6)
Cu···Cu intrachain	14.157(2)	13.851(2)	12.910(2)
Cu···Cu interchain	11.823(2), 15.292(2)	—	12.879(2), 18.674(2)
Cu···Cu intraribbon	—	9.264(2), 12.453(2)	—
Cu···Cu interribbon	—	6.219(2)	—
Cu···Cu intersheet	5.440(2), 9.504(2)	—	7.333(2), 7.361(2)
Cu···O(11)[a]	3.005(3)	2.441(3)	2.863(2)
Cu···O(21)	3.240(3)	—	—
Dihedral angle/°	6.06(13)	6.93(7)	6.55(7)

[a] O(23) for complex **8**; Cl(1) for **9**.

Table 3 Pertinent details of the hydrogen-bonded contacts in the chain structures of complexes **7**, **8** and **9**

	Symmetry code	D–H/Å	D···A/Å	H···A/Å	D–H···A/°
Complex **7**					
N(131)–H(13B)···O(22)	$1 - x, 1 - y, -z$	0.88	2.912(3)	2.10	153
N(104)–H(104)···O(22)	$1 - x, 1 - y, -z$	0.88	2.897(3)	2.07	156
N(231)–H(23B)···O(23)	$2 - x, 1 - y, 1 - z$	0.88	3.032(3)	2.22	154
N(204)–H(204)···O(21)	$2 - x, 1 - y, 1 - z$	0.88	2.785(3)	1.91	172
Complex **8**					
N(131)–H(13B)···O(13)	x, y, z	0.88	2.966(3)	2.16	152
N(104)–H(104)···O(13)	$-x, y, z$	0.88	2.873(3)	2.03	160
N(231)–H(23B)···O(12)	$0.5 + x, 0.5 - y, -0.5 + z$	0.88	3.096(3)	2.25	162
N(204)–H(204)···O(14)	$0.5 + x, 0.5 - y, -0.5 + z$	0.88	2.839(3)	1.98	164
Complex **9**					
N(131)–H(13B)···Cl(1)	$2 - x, 2 - y, 1 - z$	0.88	3.238(2)	2.41	157
N(104)–H(104)···Cl(1)	$2 - x, 2 - y, 1 - z$	0.88	3.255(2)	2.41	161
N(231)–H(23B)···Cl(1)	$1 - x, 1 - y, 1 - z$	0.88	3.274(2)	2.45	156
N(204)–H(204)···Cl(1)	$1 - x, 1 - y, 1 - z$	0.88	3.224(2)	2.40	157

Table 4 Pertinent details of the hydrogen-bonded contacts linking the chains of complexes **7**, **8** and **9**

	Symmetry code	D–H/Å	D···A/Å	H···A/Å	D–H···A/°
Complex **7**					
N(131)–H(13A)···O(12)	$1 - x, -y, -z$	0.88	2.896(3)	2.04	166
N(106)–H(106)···O(11)	$1 - x, 1 - y, 1 - z$	0.88	2.934(3)	2.10	157
N(206)–H(206)···O(11)	$1 - x, 1 - y, 1 - z$	0.88	2.931(3)	2.09	160
Complex **8**					
N(131)–H(13A)···O(22)	$1.5 - x, 0.5 + y, 0.5 - z$	0.88	2.896(3)	2.05	162
N(231)–H(23A)···O(12)	$1.5 - x, 0.5 + y, 0.5 - z$	0.88	2.869(3)	2.09	147
Complex **9**					
N(106)–H(106)···O(12)	x, y, z	0.88	2.981(2)	2.13	162
N(206)–H(206)···O(12)	x, y, z	0.88	2.872(2)	2.13	160
N(131)–H(13A)···O(2W)	$1 + x, y, 1 + z$	0.88	2.858(3)	2.07	149
N(231)–H(23A)···O(1W)	$1 + x, y, 1 + z$	0.88	2.888(3)	2.05	160
O(1W)–H(1WA)···O(11)	$-x, 1 - y, -z$	0.82	2.952(3)	2.23	148
O(1W)–H(1WB)···O(14)	x, y, z	0.82	2.759(3)	1.96	167
O(2W)–H(2WA)···O(13)	x, y, z	0.82	2.740(3)	1.94	166

separations differ markedly, that through the chain-generating methyl sulfate {Scheme 4(b); 9.504 Å} being much longer than that through the sheet-generating methyl sulfate {Scheme 4(a); 5.440 Å}.

The single weak Cu···Cl contact which completes the square pyramid in complex **9** {Fig. 1(c); Table 2} holds together pairs of sheets in a centrosymmetric fashion to give a bilayer arrangement (Fig. 6). The bilayers are connected by O–H···O

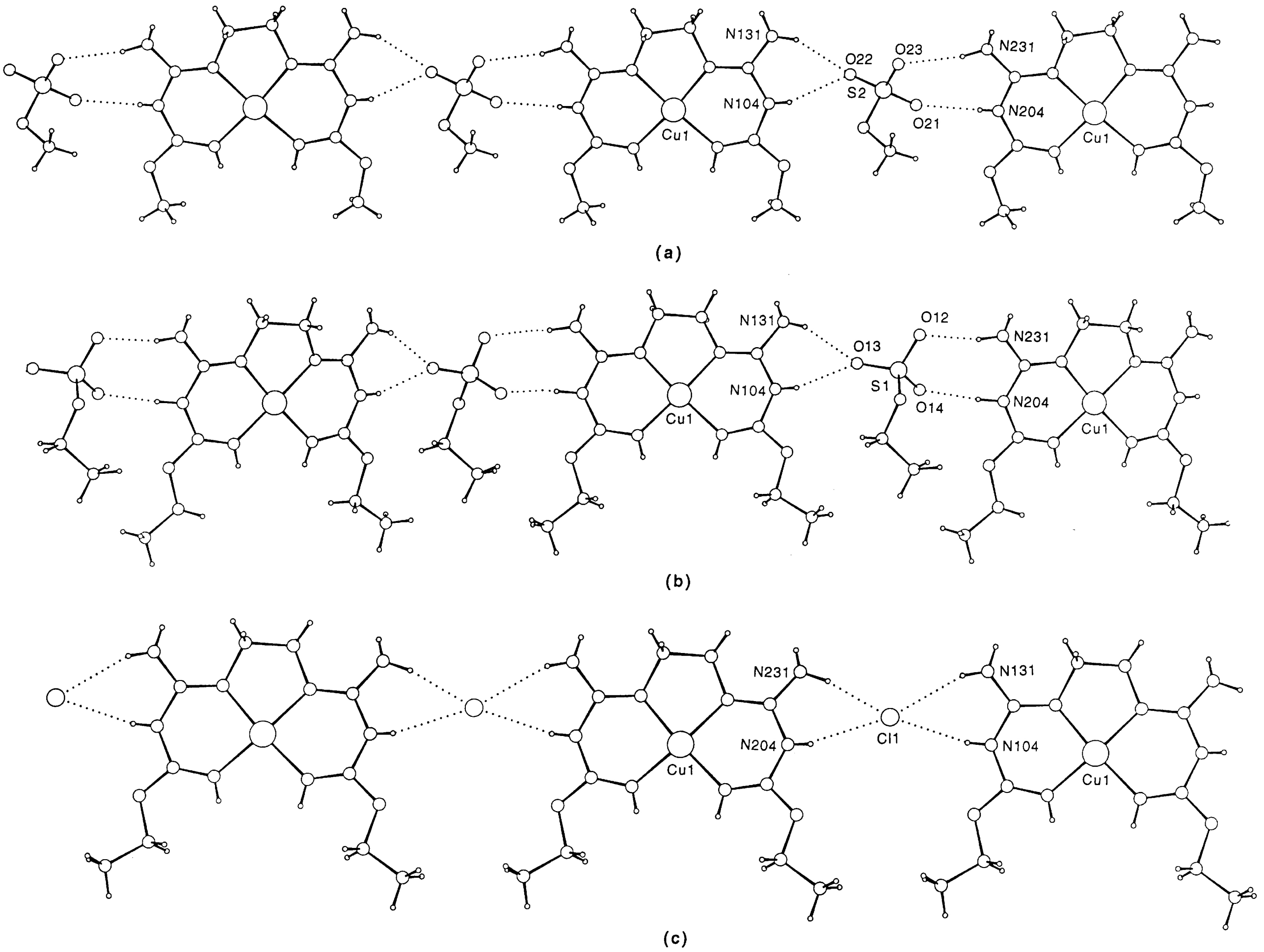

Fig. 2 Structures of the chains in (a) $[CuL^{3m}][MeOSO_3]_2$ **7**, (b) $[CuL^{3e}][EtOSO_3]_2$ **8** and (c) $[CuL^{3e}][EtOSO_3]Cl{\cdot}2H_2O$ **9** showing the hydrogen bonded supramolecular synthons.

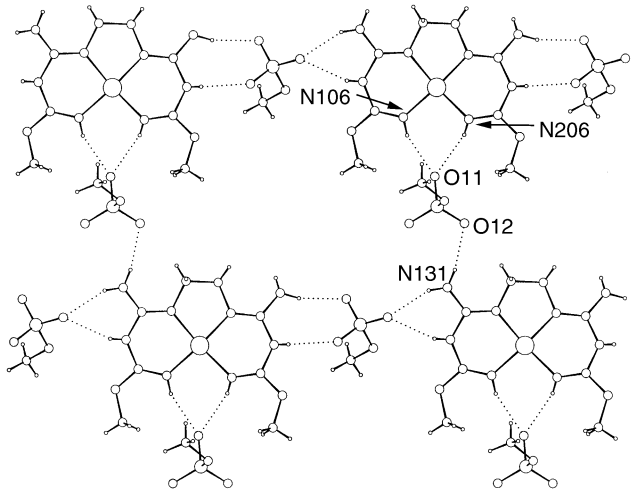

Fig. 3 Sheet structure of $[CuL^{3m}][MeOSO_3]_2$ **7**.

hydrogen bonds between water molecules (O2W) and oxygen atoms (O14) from ethyl sulfate anions in adjacent bilayers (Fig. 6; Table 5).

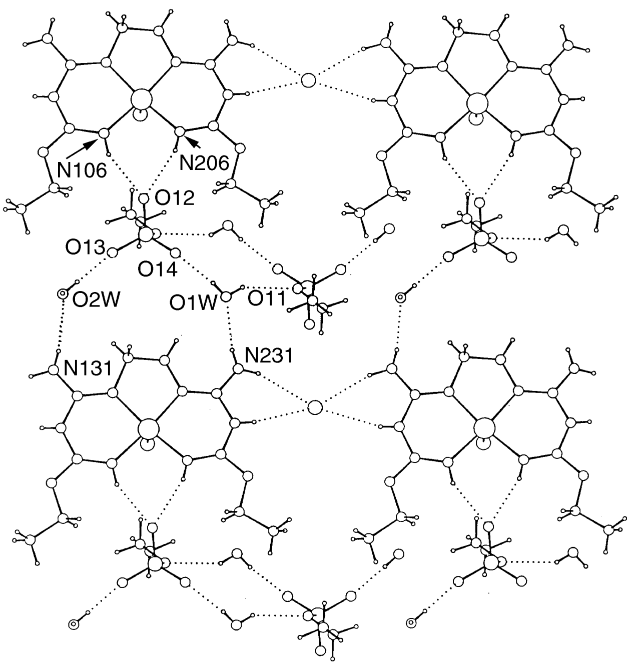

Fig. 4 Sheet structure of $[CuL^{3e}][EtOSO_3]Cl{\cdot}2H_2O$ **9**.

Construction of 3-D framework for compound 8

The sinusoidal alignment of the chains in complex **8** prevents the generation of 2-D architectures as seen in **7** and **9**. Instead a complex framework structure is formed. The chains, which propagate in the ⟨101⟩ direction, are stacked directly on top of each other (Scheme 5; full lines). A second set of chains (Scheme 5; dashed lines) is linked to the first set to form a bilayered arrangement. The two sets of chains, which face in opposite directions {Fig. 7(a)}, are connected through two N–H···O hydrogen bonds at their peaks and troughs {Fig. 7(a) and 7(b)}. Full details of the hydrogen-bonding network is in Table 4. Although N231–H23A···O12 can be seen in Fig. 7, N131–H13A···O22 is not shown as O(22) forms part

Table 5 Pertinent details of the hydrogen-bonded contacts generating the 3-D structure of complexes **7**, **8** and **9**

	Symmetry code	D–H/Å	D···A/Å	H···A/Å	D–H···A/°
Complex **7**					
N(231)–H(23A)···O(23)	*x*, −1 + *y*, *z*	0.88	3.015(3)	2.24	147
Complex **8**					
N(106)–H(106)···O(24)	1 − *x*, −*y*, −*z*	0.88	3.044(3)	2.20	160
N(206)–H(206)···O(24)	1 − *x*, −*y*, −*z*	0.88	2.996(3)	2.13	166
Complex **9**					
O(2W)–H(2WB)···O(14)	−*x*, 2 − *y*, −*z*	0.82	2.854(3)	2.13	149

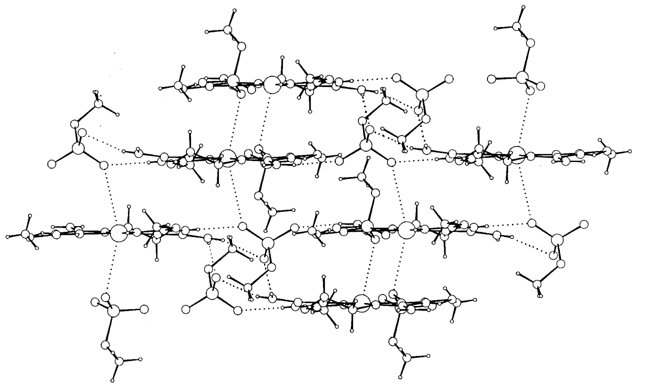

Fig. 5 Parallel packing of the sheets in $[CuL^{3m}][MeOSO_3]_2$ **7** showing the co-ordinative and hydrogen-bonding interactions involved in the generation of the framework structure.

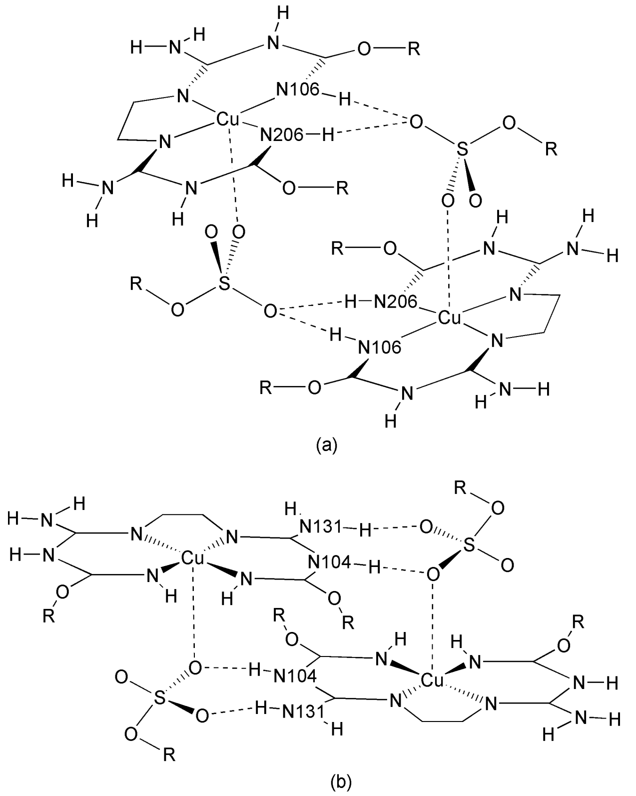

Scheme 4 Co-ordinative and hydrogen-bonding interactions linking copper(II) centres and hence sheets in compound **7** through (a) the co-ordinated imino (N106, N206) nitrogens and (b) the amino/imino (N131/N104) pair.

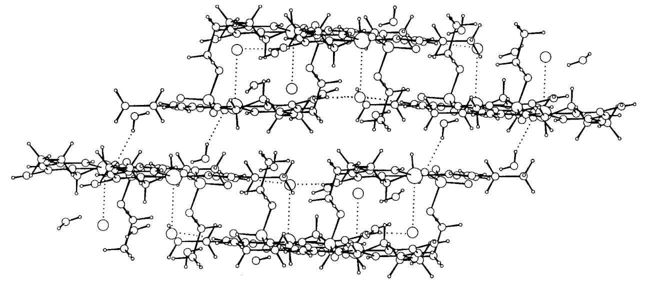

Fig. 6 Parallel packing of the sheets in $[CuL^{3e}][EtOSO_3]Cl\cdot 2H_2O$, **9** showing the co-ordinative interactions involved in the generation of the framework structure.

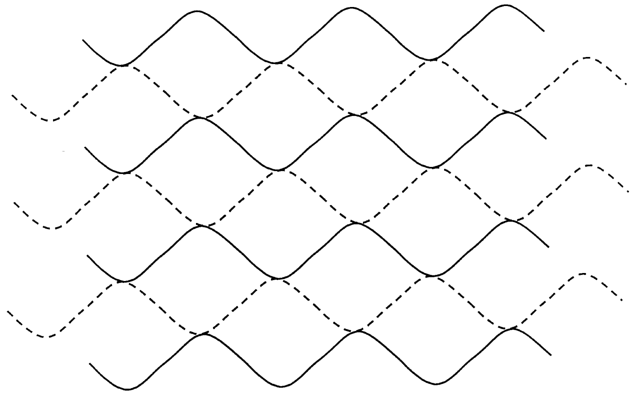

Scheme 5 The alignment of the sinusoidal chains in complex **8**. Two sets (full lines and dashed lines) of stacked chains are linked, at their peaks and troughs, through hydrogen-bonding interactions to form a bilayered arrangement.

of the co-ordinated ethyl sulfate anion which has been omitted for clarity. The principal connection between bilayers is similar to that depicted in Scheme 4(a) for compound **7**. Two ethyl sulfate anions form a centrosymmetric bridge between two $[CuL^{3e}]^{2+}$ cations, forming a co-ordinate bond to the copper centre of the first cation and a pair of hydrogen bonds to the co-ordinated imino nitrogens of the second cation. The Cu···Cu separation thus generated (6.219 Å) is marginally longer than that of the corresponding link in **7** (5.440 Å).

Conclusion

Refluxing the C_2-linked bis(2-cyanoguanidine) L^1 in methanol or ethanol containing copper(II) sulfate results, not only in the copper(II)-templated solvolysis of L^1 and concomitant formation of the $[CuL^i]^{2+}$ (i = 3m or 3e) cation, but also in the esterification of the sulfate anion to form the monoalkyl sulfate anion. The former reaction was anticipated by analogy with the corresponding reactions with copper(II) chloride[5] but the latter was quite unexpected.

The formation of alkyl sulfate is attributed to a process similar to that proposed for the generation of the $[BF_2(OMe)_2]^-$ anion in the crystallisation of $[CuL^{3e}][BF_2(OMe)_2][BF_4]$.[5] The $[ROSO_3]^-$ anion has the appropriate geometry and hydrogen-bonding acceptor properties to link $[CuL^i]^{2+}$ cations and form a supramolecular synthon {Scheme 6(a)} comparable with those found in the corresponding chloride {Scheme 6(b); **1**–**4**} and difluorodimethoxoborate {Scheme 6(c); **5**} compounds.

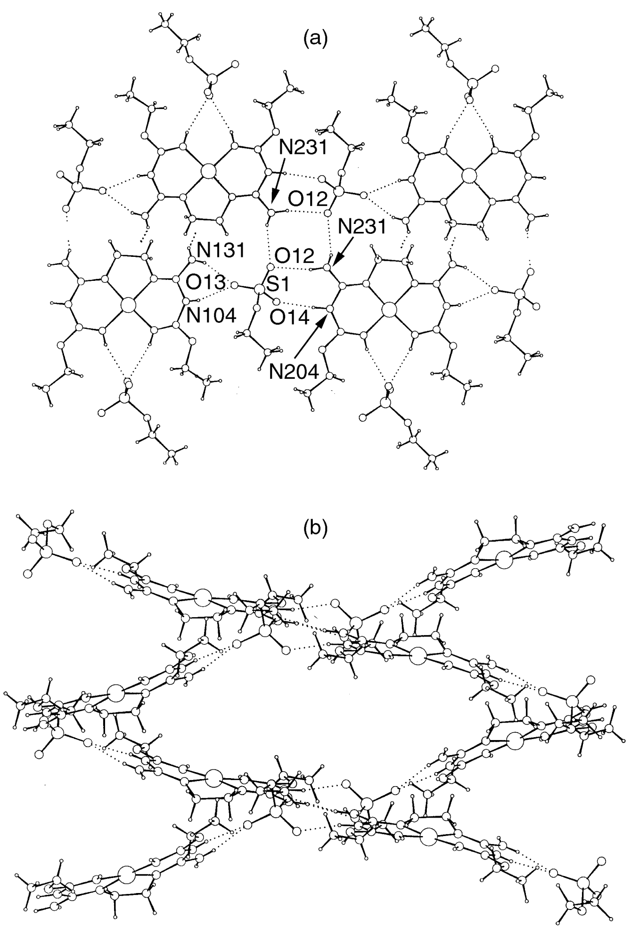

Fig. 7 Views of the structure of [CuL^{3e}][EtOSO$_3$]$_2$ **8** perpendicular to the 010 plane (a) and the 101 plane (b) showing the hydrogen-bonding contacts (a) linking the sinusoidal chains (b).

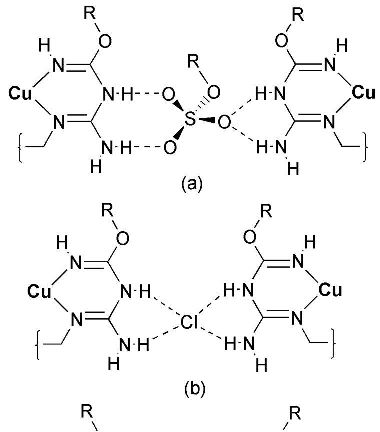

Scheme 6 Hydrogen-bonded supramolecular synthons generating the chains of alternating cations and anions in (a) the alkyl sulfates, (b) the chlorides and (c) the difluorodimethoxoborates.

The esterification equilibria (1) will exist in all alcoholic media containing sulfate, albeit with very small equilibrium constants. Owing to the match between [CuL^{i}]$^{2+}$ cation and [ROSO$_3$]$^-$ anion, the product containing the supramolecular synthon will crystallise/precipitate from solution, despite the low anion concentration. As this process progresses the anion is removed from solution disturbing the equilibrium. Thus as alkyl sulfate is utilised in the formation of the supramolecular structure the system will respond constantly generating more anion and hence increasing amounts of product.

When a mixture of anions (chloride and ethyl sulfate) is present in the crystallisation medium the preferred chain supramolecular synthon is that containing chloride. The ethyl sulfate anions are involved, together with water molecules, in a complex hydrogen-bonding network which connects the chains into sheets. Under these circumstances the two major hydrogen-bonding donor sites on the [CuL^{i}]$^{2+}$ cation act as anion recognition centres, the amino/imino pairs (N131/N104; N231/N204) binding the chloride and the pair of co-ordinated imino nitrogens (N106/N206) binding the alkyl sulfate.

Experimental

All chemical reagents were purchased from Aldrich Chemical Company Ltd. and used without further purification. 1,2-Bis(2-cyanoguanidino)ethane, L^1, was prepared from 1,2-diaminoethane and sodium dicyanamide as described previously.[5] Elemental (C, H, N) analytical data and mass spectra were obtained using a Perkin-Elmer 240B elemental analyser and a VG70E micromass spectrometer by Mr T. Spencer and Mr T. Hollingworth, respectively, of the Nottingham University School of Chemistry Analytical Services Group. Infrared spectra were obtained on a Perkin-Elmer PE983G spectrometer as KBr pressed pellets, UV-Visible spectra on a UNICAM UV1 UV-Vis spectrophotometer, and EPR spectra on a Bruker EMX X-Band EPR spectrometer.

Preparations

[CuL^{3m}][MeOSO$_3$]$_2$ 7. CuSO$_4$·5H$_2$O (0.250 g; 1 × 10^{-3} mol) and L^1 (0.194 g; 1 × 10^{-3} mol) were dissolved in methanol (50 cm^3). The mixture was refluxed overnight to give a purple solution over a pale blue solid. The solvent was cooled and filtered to remove the excess of solid. A purple precipitate was formed after reduction in solvent volume. Yield: 0.060 g; 0.11 × 10^{-3} mol; 11%. Found (calc. for $C_{10}H_{24}CuN_8O_{10}S_2$): C 22.00 (22.05); H 4.45 (4.40); N 20.50 (20.60)%. IR (ν/cm^{-1}): 3416ms; 3301ms; 3214ms; 3124mw; 3058mw; 2986mw; 2899mw; 1679s; 1560ms; 1459w; 1410w; 1375w; 1217ms, br; 1179mw; 1061mw; 1002mw; 959w; 813vw; 754mw; 609w; 579w; 553vw and 497w. FAB MS (m/z): 320, [Cu(L^{3m} − H)]$^+$. UV-Vis (in MeOH): λ_{max} 546 nm (ε = 61.21 dm^3 mol^{-1} cm^{-1}). Crystals suitable for X-ray diffraction study were obtained by vapour phase diffusion of Et$_2$O into a MeOH solution of the product.

[CuL^{3e}][EtOSO$_3$]$_2$ 8. CuSO$_4$·5H$_2$O (0.250 g; 1 × 10^{-3} mol) and L^1 (0.194 g; 1 × 10^{-3} mol) were dissolved in ethanol (50 cm^3). The mixture was refluxed overnight to give a purple solution over a pale blue solid. The solvent was cooled, filtered to remove the excess of solid and reduced in solvent volume. After five days a purple precipitate was formed. Yield: 0.090 g; 0.15 × 10^{-3} mol; 15%. Found (calc. for $C_{14}H_{32}CuN_8O_{10}S_2$): C 27.75 (28.00); H 5.20 (5.30); N 18.70 (18.65)%. IR (ν/cm^{-1}): 3411s; 3342s; 3290s; 3241s; 2989ms; 2906mw; 1682vs; 1559s; 1437mw; 1390mw; 1369ms; 1242vs; 1207vs 1177s; 1112mw; 1062ms; 1017s; 944w; 910ms; 882mw; 778ms; 760ms; 731mw; 621mw; 582ms; 565w and 516w. FAB MS (m/z): 348, [Cu(L^{3e} − H)]$^+$. UV-Vis (in MeOH): λ_{max} 543 nm (ε = 55.01 dm^3 mol^{-1} cm^{-1}). Crystals suitable for X-ray diffraction study were obtained by vapour phase diffusion of Et$_2$O into a MeOH solution of the product.

[CuL^{3e}][EtOSO$_3$]Cl·2H$_2$O 9. Crystals suitable for X-ray diffraction study were obtained by slow evaporation of a MeOH solution (6 cm^3) containing an equimolar mixture of [CuL^{3e}][EtOSO$_3$]$_2$ (0.029 g, 5.0 × 10^{-5} mol) and [CuL^{3e}]Cl$_2$·2H$_2$O (0.022 g, 5.0 × 10^{-5} mol). Yield: 0.025 g; 4.59 × 10^{-5} mol; 92%.

Table 6 Crystallographic data for complexes **7**, **8** and **9**

	7	**8**	**9**
Formula	$C_{10}H_{24}CuN_8O_{10}S_2$	$C_{14}H_{32}CuN_8O_{10}S_2$	$C_{12}H_{31}ClCuN_8O_8S$
M	544.03	600.14	546.5
Crystal system	Triclinic	Monoclinic	Triclinic
Space group	$P\bar{1}$	$P2_1/n$	$P\bar{1}$
a/Å	10.097(1)	14.246(2)	8.3861(7)
b/Å	10.143(1)	8.2144(11)	11.791(1)
c/Å	11.550(1)	21.292(3)	12.552(1)
α/°	114.325(2)	—	93.835(2)
β/°	98.612(2)	100.214(2)	108.332(2)
γ/°	98.146(2)	—	104.004(2)
U/Å^3	1038.2(3)	2452.2(8)	1129.3(3)
Z	2	4	2
μ (Mo-Kα)/mm^{-1}	1.321	1.127	1.233
Reflections: unique; observed; R_{int}	4835; 3707; 0.049	5520; 3831; 0.072	5213; 4572; 0.031
$wR2$ (all data); R ($I \geq 2\sigma(I)$)	0.1072; 0.0411	0.0837; 0.0387	0.0842; 0.0297

Found (calc. for $C_{12}H_{31}ClCuN_8O_8S$): C 26.65 (26.35); H 5.15 (5.70); N 20.65 (20.50)%. IR (ν/cm^{-1}): 3446m; 3380m; 3320m; 3199m; 3057w; 2986mw; 1676vs; 1569s; 1438mw; 1364mw; 1236m; 1184ms; 1114w; 1063w; 1013ms; 913w; 772mw; 704w; 624w; 582w and 515w. FAB MS (m/z): 348, $[Cu(L^{3e} - H)]^+$.

X-Ray data collection and structure determination

X-Ray diffraction data were collected at 150 K for complexes **7**, **8** and **9** using a Stoë IPDS image plate diffractometer equipped with an Oxford Cryosystem open flow cryostat.[13] Absorption corrections were applied for all complexes either numerically or using XABS 2.[14] The structures were solved by direct methods using SHELXS 97[15] and refined by full matrix least squares using SHELXL 97.[16] All hydrogen atoms, including those of the water molecules in **9**, were found in Fourier difference syntheses. Those of the methylene, methyl, imino and amino groups were subsequently placed in geometrically calculated positions and thereafter refined using a riding model {C–H 0.96; N–H 0.88; O–H 0.82 Å; $U_{iso}(H) = 1.2U_{eq}(X)$}. All non-hydrogen atoms were refined with anisotropic displacement parameters. Crystal data and details of structure solutions are summarised in Table 6. All structure diagrams were generated using CAMERON.[17]

CCDC reference number 186/2061.

See http://www.rsc.org/suppdata/dt/b0/b003427o/ for crystallographic files in .cif format.

Acknowledgements

We thank the EPSRC for the provision of a diffractometer and the Royal Thai Government for financial support (to U. S.).

References

1 J. C. M. Rivas and L. Brammer, *Coord. Chem. Rev.*, 1999, **183**, 43; S. K. Shawla, *Indian J. Chem., Sect. A*, 1997, **36**, 729; A. D. Burrows, S. Menzer, D. M. P. Mingos, A. J. P. White and D. J. Williams, *J. Chem. Soc., Dalton Trans.*, 1997, 4237; M. Munakata, L. P. Wu and T. Kuroda-Sowa, *Bull. Chem. Soc. Jpn.*, 1997, **70**, 1727; A. D. Burrows, D. M. P. Mingos, A. J. P. White and D. J. Williams, *J. Chem. Soc., Dalton Trans.*, 1996, 3805; *Chem. Commun.*, 1996, 97; M. M. Chowdhry, D. M. P. Mingos, A. J. P. White and D. J. Williams, *Chem. Commun.*, 1996, 899; J. E. McGrady and D. M. P. Mingos, *J. Chem. Soc., Perkin Trans. 2*, 1996, 3805; L. Brammer, D. Zhao, F. T. Lapido and J. Braddockwilking, *Acta Crystallogr., Sect. B*, 1995, **51**, 632; A. D. Burrows, C. W. Chan, M. M. Chowdhry, J. E. McGrady and D. M. P. Mingos, *Chem. Soc. Rev.*, 1995, **24**, 329.

2 A. S. Batsanov, M. J. Begley, M. W. George, P. Hubberstey, M. Munakata, C. E. Russell and P. H. Walton, *J. Chem. Soc., Dalton Trans.*, 1999, 4251; A. J. Blake, P. Hubberstey, W.-S. Li, C. E. Russell, B. J. Smith and L. D. Wraith, *J. Chem. Soc., Dalton Trans.*, 1998, 747; A. S. Batsanov, P. Hubberstey, C. E. Russell and P. H. Walton, *J. Chem. Soc., Dalton Trans.*, 1997, 2667.

3 M. C. T. Fyfe and J. F. Stoddart, *Coord. Chem. Rev.*, 1999, **183**, 139; A. Nangia and G. R. Desiraju, *Top. Curr. Chem.*, 1998, **198**, 57; G. R. Desiraju, *Curr. Opin. Solid State Mater. Sci.*, 1997, **2**, 451; *Angew. Chem., Int. Ed. Engl.*, 1995, **34**, 2311; S. Subramanian and M. J. Zaworotko, *Coord. Chem. Rev.*, 1994, **137**, 357.

4 A. J. Blake, N. R. Champness, P. Hubberstey, W.-S. Li, M. Schröder and M. A. Withersby, *Coord. Chem. Rev.*, 1999, **183**, 117; S. R. Batten and R. Robson, *Angew. Chem., Int. Ed.*, 1998, **37**, 1460; N. R. Champness and M. Schröder, *Curr. Opin. Solid State Mater. Sci.*, 1998, **3**, 419; O. M. Yaghi, H. Li, C. Davis, D. Richardson and T. L. Groy, *Acc. Chem. Res.*, 1998, **31**, 474.

5 P. Hubberstey, U. Suksangpanya and C. L. Wilson, *J. Chem. Soc., Dalton Trans.*, paper no. b004593o.

6 D. Akrivos, S. K. Hadjikakou, P. Karagiannidis, M. Luic and B. Kojicprodic, *J. Coord. Chem.*, 1994, **31**, 273.

7 T. M. Vimala and S. Swaminathan, *Curr. Sci.*, 1969, **38**, 362.

8 D. A. Baldwin, J. C. A. Boeyens, R. G. Copperthwaite, J. H. N. Loubser and A. J. Markwell, *J. Crystallogr. Spectrosc. Res.*, 1984, **14**, 157.

9 F. R. Keene, D. J. Azalde and T. A. Wilson, *Inorg. Chem.*, 1987, **26**, 2211.

10 H. Werner, O. Schippel, J. Wolf and M. Schulz, *J. Organomet. Chem.*, 1991, **417**, 149.

11 R. E. Gerkin and W. J. Reppert, *Acta Crystallogr., Sect. C*, 1984, **40**, 781; C. R. Hubbard, C. O. Quicksall and R. A. Jacobson, *Acta Crystallogr., Sect. B*, 1974, **30**, 2613; R. W. Broach, J. M. Williams, G. P. Felcher and D. G. Hinks, *Acta Crystallogr., Sect. B*, 1979, **35**, 2317.

12 See, for example, J. M. Dixon and M. Kelly, *Int. J. Mod. Phys.*, 1997, **11**, 3033, 3049; H. P. Moll, J. vanTol, P. Wyder, M. S. Tagirov and D. A. Tayurskii, *Phys. Rev. Lett.*, 1996, **66**, 3459.

13 J. Cosier and A. M. Glazer, *J. Appl. Crystallogr.*, 1986, **19**, 105.

14 S. Parkin, B. Moezzi and H. Hope, *J. Appl. Crystallogr.*, 1995, **28**, 53.

15 G. M. Sheldrick, SHELXS 97, *Acta Crystallogr., Sect. A*, 1990, **46**, 467.

16 G. M. Sheldrick, SHELXL 97, University of Göttingen, 1997.

17 D. J. Watkin, C. K. Prout and L. J. Pearce, CAMERON, Chemical Crystallography Laboratory, University of Oxford, 1996.